energy&fuels

pubs.acs.org/EF Article

Improving the Immobilization of Glucose Oxidase on Carbon Cloth Via a Hybrid Approach of Cross-Linked Chitosan/TPP Matrices with Na Polymers for High-Performance Self-Pumping Enzyme-Based Biofuel Cells

Ngoc Bich Duong, Van Men Truong, Yi-Shiuan Li, Chih-Liang Wang,* and Hsiharng Yang*

Cite This: *Energy Fuels* 2020, 34, 10050−10058 Read Online

ACCESS | Metrics & More | Article Recommendations | Supporting Information

ABSTRACT: The real-world application of an enzyme-based biofuel cell (EBFC) requires the desirable immobilization of enzymes on the electrode surface, offering the feasibility of addressing its short lifetime and low-power density. Nevertheless, an efficient immobilization of enzymes strongly relies on the preferred scaffolding between the enzyme and the electrode. Accordingly, the development of a promising route to attain a tunable scaffold structure is urgently required. Herein, we present a facile and ecofriendly route for efficiently controlling the scaffold structure by investigating the interplay of tripolyphosphate (TPP), chitosan (CS), and Na. A series of glucose oxidase (GOx)-based anodic electrodes, GOx[CS/TPP]CC, GOx[CS/Na]CC, and GOx[CS/TPP/Na]CC, are synthesized using CS/TPP, CS/Na, and CS/TPP/Na as the scaffolding on carbon cloth (CC) followed by the immobilization of GOx for a comparative study of the microstructure, enzyme loading, and electrochemical property. It is revealed that the self-pumping EBFC, driven by capillary force, utilizing GOx[CS/TPP/Na]CC can deliver a higher peak power density (1.077 mW cm^{-2}) than that utilizing GOx[CS/TPP]CC (0.776 mW cm^{-2}) and GOx[CS/Na]CC (0.682 mW cm^{-2}). The self-pumping EBFC utilizing GOx[CS/TPP/Na]CC can retain 89.2% of its beginning performance even after 240 h of testing, as compared with that utilizing GOx[CS/Na]CC (61.1%). This enhancement can be attributed to the formation of a desirable scaffold structure via the cross-linked CS/TPP matrices combined with Na polymers for the hybrid enzyme immobilization, simultaneously offering the capability of improving the enzyme-loading efficiency, facilitating the interaction between the surface electrode and the enzyme, and preventing the release of the enzyme during the cell operation.

1. INTRODUCTION

The rapid development of the global economy has driven the demand for the power generation. However, the majority of our energy supply comes from the combustion of fossil fuel that emits carbon dioxide,[1] subsequently causing global warming.[2] Enzyme-based biofuel cells (EBFCs), one sort of fuel cells that can convert an ecofriendly biological source into electrical energy by utilization of the enzyme as a catalyst instead of expensive metals, has been regarded as an alternative choice recently.[3−5] The EBFCs have certain benefits on the basis of the features of enzymes.[6] For instance, the high specificity toward the respective substrate enables them to operate in a complex medium. The high catalytic ability can also be exhibited under low temperature, neutral pH, and normal pressure.[7,8] The overpotential for an electrocatalytic reaction required at the anode or cathode is relatively low. These inherent advantages have spawned versatile applications of EBFCs, such as in portable devices,[9] implantable biofuel cells,[10−12] self-powered biosensors,[13] and self-powered biomolecular keypad lock security systems.[14]

The schematic diagram of a simple EBFC utilizing the commonly used enzyme of glucose oxidase (GOx) is illustrated in Figure 1. During the operation, glucose is oxidized into gluconolactone,[15] which is hydrolyzed into gluconic acid[16] through the catalytic activity of a GOx enzyme, as shown in the reaction below, along with the generation of an electron and a proton.

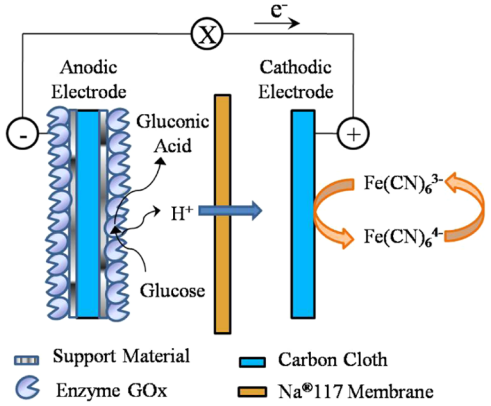

Figure 1. Schematic diagram of a simple EBFC.

Received: March 31, 2020
Revised: July 1, 2020
Published: July 2, 2020

https://dx.doi.org/10.1021/acs.energyfuels.0c01033
Energy Fuels 2020, 34, 10050−10058

$$C_6H_{12}O_6 + H_2O \xrightarrow{GOx} C_6H_{12}O_7 + 2e^- + 2H^+ \quad (1)$$

On the other hand, the reduction of oxygen into water, involving the redox of ferricyanide ($Fe[CN]_6^{3-}$)/ferrocyanide ($Fe[CN]_6^{4-}$), happens by receiving the electron and proton at the cathode, as given by the following reactions.[17,18]

$$2Fe(CN)_6^{3-} + 2e^- \rightarrow 2Fe(CN)_6^{4-} \quad (2)$$

$$2Fe(CN)_6^{4-} + 2H^+ + 1/2O_2 \rightarrow 2Fe(CN)_6^{3-} + H_2O \quad (3)$$

Total

$$C_6H_{12}O_6 + 1/2O_2 \rightarrow C_6H_{12}O_7 \quad (4)$$

Though EBFCs based on concepts similar to those described above have been demonstrated, pushing them into real applications remains challenging because of their limited lifetime and low power density. It is worth noting that the redox enzymes usually have the natural property of their catalytic sites being buried in protein shells, making the enzyme activity vulnerable to their immobilized situation on the electrode.[19,20] Accordingly, the enzyme properly immobilized on the surface of the electrode plays a critical part in the EBFC performance as well as its longevity.

Previous studies of GOx immobilized on a bioelectrode have proposed various characteristics, such as physical adsorption,[21−25] chemical covalence,[26,27] polymer entrapment,[28,29] and cross-linking.[30] Among them, the cross-linking characteristic, enabling to offer a stable function to prevent the enzymes from leaching, is particularly a facile and efficacious way for enzyme immobilization on the electrode surface with high stability.[31] However, the tendency of poorly controlled aggregation becomes a hurdle for the diffusion of the substrate into the cross-linked enzyme structure. The active sites of GOx can also be covered by the cross-linker, blocking the glucose from proceeding the reaction.[26] In addition, though some commonly used cross-linkers like the glutaraldehyde (GA) can bring some advantages such as low cost, high throughput, and easy treatment,[26,32] they are toxically strong irritants and sterilants, potentially unfriendly toward the required biocompatible environment of implantable battery-powered and microscale devices.[33]

Chitosan (CS) is a functional material that is commonly used as a supporting scaffold for the immobilization of a GOx enzyme to apply in biosensors[34,35] and biofuel cells[36−39] due to its biocompatible and nontoxic advantages. The immobilization of GOx on a CS-coated electrode can also exhibit a speedy heterogeneity of electron transfer between the oxidation/reduction center of the GOx enzyme and the electrode.[40] Accordingly, the feasibility of CS cross-linked with other agents has been explored by numerous studies in various fields. The CS nanoparticles can be prepared with tripolyphosphate (TPP) as a cross-linking agent for the encapsulation of tacrine.[41] Liu et al. used TPP cross-linked CS membranes for the removal of humic acid.[42] Shrestha et al. presented the cross-linking of CS with GOx immobilized on a PPy/Nafion/fMWCNT bionanohybrid film for a high-performance glucose biosensor.[43] Though the above-mentioned studies demonstrated several possibilities of CS cross-linking, studies on GOx immobilized on a CS cross-linking-based scaffold on the electrode surface remain few. Accordingly, this study aims to investigate a new design of a biocatalyst that combines TPP cross-linked CS with a Na polymer to form a tunable scaffold structure for immobilizing GOx on CC (GOx[CS/TPP/Na]CC). To understand the effect of TPP, Na, and CS on the immobilization of GOx on CC, different samples of GOx[CS/TPP]CC, GOx[CS/Na]CC, and GOx[CS/TPP/Na]CC were prepared for a comparative study. GOx[CS/TPP/Na]CC sample shows a high loading of GOx on CC and a great catalytic property because the porous structure of the scaffold formed by the combination of cross-linked CS/TPP matrices with Na polymers can not only help prevent the release of the enzyme but also facilitate the uniform dispersion of the GOx enzyme loading during the process of immobilization.

On the other hand, to circumvent the need for the extra power supply and space in the lightweight and portable cell,[12,44−48] a so-called self-pumping design of a flow plate channel and an end plate that allows the fuels to automatically flow by capillary force is utilized to evaluate the performance of a series of synthesized biocatalysts.[49,50] Our study result indicates that the self-pumping EBFC utilizing GOx[CS/TPP/Na]CC can deliver the highest peak power density (1.077 mW cm^{-2}) as compared with that utilizing GOx[CS/TPP]CC (0.776 mW cm^{-2}) and GOx[CS/Na]CC (0.682 mW cm^{-2}). In addition, the self-pumping EBFC utilizing GOx[CS/TPP/Na]CC can retain 89.2% of its beginning performance even after 240 h of stable testing.

2. EXPERIMENTAL SECTION

2.1. Reagents. Chitosan with high molecular weight (MW 140 000 dal/mol, 90% deacetylation), which is sieved by a 100 mesh filter, was bought from Shin ERA Tech. Co., Ltd. in Taiwan. Glucose oxidase from *Aspergillus niger* (Gluzyme Mono 10 000 BG) was purchased from Novo Nordisk Bioindustrials Inc. in Denmark. Carbon cloth (CC) was bought from CETECH Co., Ltd. in Taiwan. A Nafion perfluorinated solution containing 15−20% water (Na), sodium tripolyphosphate (TPP), 1-ethyl-3-(3-dimethylaminopropyl)-carbodiimide (EDC), and potassium hexacyanoferrate III ($K_3[Fe(CN)_6]$) were purchased from Sigma-Aldrich. *N*-hydroxysuccinimide (NHS) was obtained from Alfar Aesar. A Nafion 117 membrane obtained from DuPont was thermally treated with H_2O_2 and H_2SO_4.[51]

2.2. Fabrication of Bioanodic Electrodes. *2.2.1. GOx[CS/TPP]CC Electrode.* To prepare the GOx[CS/TPP]CC electrode, first 0.5 g of CS was dissolved in 50 mL of deionized water (DI) with 1% (v/v) acetic acid (CH_3COOH) under magnetic stirring to form a CS solution. Second, 12.5 mg of TPP was dissolved in 12.5 mL of DI water and then added in the CS solution under magnetic stirring for 30 min at room condition to form the cross-linked [CS/TPP] scaffold. The formation of the [CS/TPP] scaffold is based on the physical interaction between the positively charged (NH_3^+) of CS and negatively charged phosphoric ions (PO_3^-) of TPP, as shown in Figure S1. A small piece of CC (3 x 2 cm^2, 131.5 mg) was soaked into the mixed solution of [CS/TPP], followed by an ultrasonic agitation for 30 min. To precipitate CS, the [CS/TPP]CC was transferred into a 1 M NaOH solution. Afterward, the as-prepared [CS/TPP]CC electrode was put into DI water for 3 h to wash off the remaining NaOH solution and this washing step was repeated three times. Finally, the bioanodic electrode of GOx[CS/TPP]CC was prepared by placing the [CS/TPP]CC into the activated GOx solution and agitating for 1 h at 120 rpm. The complete GOx[CS/TPP]CC electrode was stored in DI water before the assembly of the EBFC. The activated GOx solution was first prepared for the enzyme activation by adding 394.5 mg of GOx in 50 mL of phosphate-buffered saline (PBS) (pH 6) with 25 mg of EDC (2.6 mM) and agitating for 1 h at 120 rpm. The mixture was then added to 30 mg of NHS (5.2 mM), followed by agitating for 1 h at 120 rpm to prevent the enzyme reduction and improve the stability of the active ester.[52] More details are shown in Figure S2.

2.2.2. GOx[CS/Na]CC Electrode. To prepare the GOx[CS/Na]CC electrode, 0.5 g of CS was dissolved in 50 mL of DI water added with

https://dx.doi.org/10.1021/acs.energyfuels.0c01033
Energy Fuels 2020, 34, 10050−10058

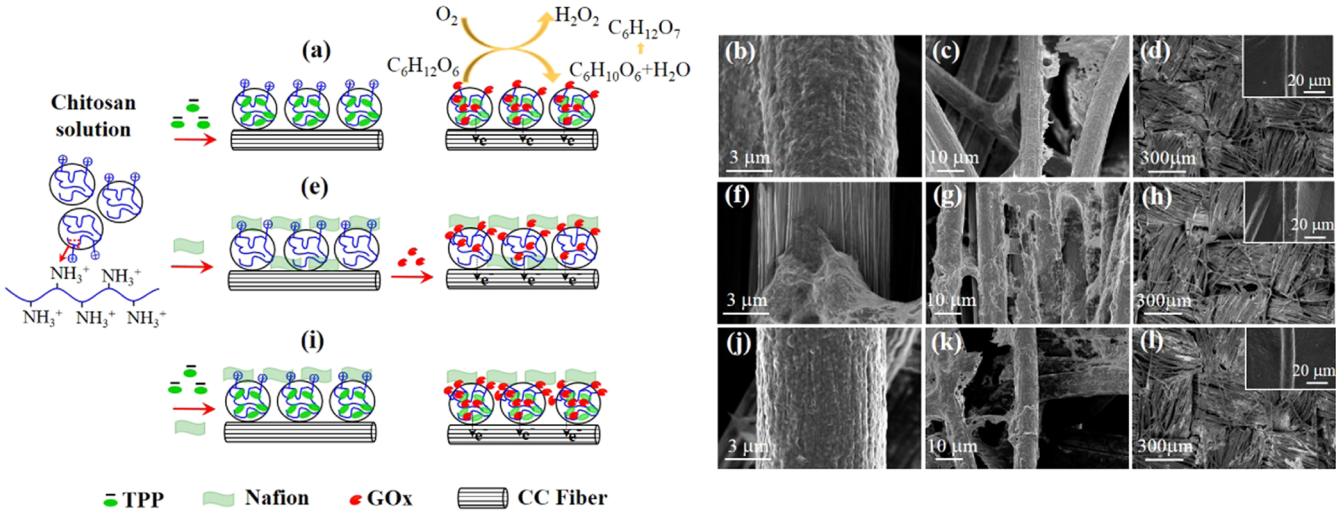

Figure 2. Schematic depiction of the different bioanodic electrodes of (a) GOx[CS/TPP]CC, (e) GOx[CS/Na]CC, and (i) GOx[CS/TPP/Na]CC. The corresponding SEM images at various magnifications: (b, c) [CS/TPP]CC scaffold and (d) GOx[CS/TPP]CC; (f, g) [CS/Na]CC scaffold and (h) GOx[CS/Na]CC]; (j, k) [CS/TPP/Na]CC scaffold, and (l) GOx[CS/TPP/Na]CC. The inset of (d), (h), and (l) shows a high magnification of GOx[CS/TPP]CC], GOx[CS/Na]CC, and GOx[CS/TPP/Na]CC, respectively.

1% (v/v) CH_3COOH under magnetic stirring, followed by addition of 1.5 mL of Na solution and continuous stirring at room temperature for 30 min. A small piece of CC (3 x 2 cm^2) was immersed into the mixed solution of [CS/Na], followed by ultrasonic agitation for 30 min. To precipitate CS, the [CS/Na]CC was transferred into a 1 M NaOH solution. Afterward, the as-prepared [CS/Na]CC electrode was put into DI water for 3 h to wash off the remaining NaOH solution and this washing step was repeated three times. The bioanodic electrode of GOx[CS/Na]CC was prepared by placing the [CS/Na]CC into the activated GOx solution, followed by agitating for 1 h at 120 rpm and storing in DI water before the assembly of the EBFC. The activated GOx solution was prepared in the same way.

2.2.3. GOx[CS/TPP/Na]CC Electrode. To prepare the GOx[CS/TPP/Na]CC electrode, first the CS solution was prepared by dissolving 0.5 g of CS in 50 mL of DI water added with 1% (v/v) CH_3COOH under magnetic stirring. TPP (12.5 mg) was added to 12.5 mL of deionized water (DI) and then mixed with the CS solution, followed by addition of the Na solution and stirring for 30 min at room temperature. A series of [CS/TPP/Na] solutions with 1−4% Nafion content can be prepared by adding 0.5-2.0 mL of Na solutions to the mixed solution of CS and TPP.

Next, a small piece of CC (3 x 2 cm^2) was soaked in the mixed solution of [CS/TPP/Na], followed by an ultrasonic agitation for 30 min. To precipitate CS, the [CS/TPP/Na]CC was then transferred into a 1 M NaOH solution. Afterward, the as-prepared [CS/TPP/Na]CC electrode was immersed into DI water for 3 h to wash off the remaining NaOH solution and this washing step was repeated three times. The bioanodic electrode of GOx[CS/TPP/Na]CC was prepared by placing the [CS/TPP/Na]CC into the activated GOx solution, followed by agitating at 120 rpm for 1 h and storing in DI water before the assembly of the EBFC. The activated GOx solution was prepared in the same way.

2.3. Design of a Self-Pumping EBFC. The scheme of a single EBFC system using the GOx[CS/TPP]CC, GOx[CS/Na]CC, and GOx[CS/TPP/Na]CC is displayed in Figure S3. To circumvent the typical EBFC system using an external pump for the fuel flow, a self-pumping EBFC stack (Figure S4), composed of the design of flow channel plates (Figure S5) and the top/bottom end plates (Figure S6), to drive the fuel by capillary force was utilized as mentioned in the refs 49, S3. There were three reservoirs (REs) on the top/bottom end plates (Figure S6). As the cell was operated, the fuel was manually supplied to the RE1 while the RE2 and RE3 were filled with cotton as a self-driven source so that the capillary force is generated. Based on the capillary effect, the fuel stored in the RE1 automatically flowed into RE2 and then reached the inlet of the flow channel plates at the anode/cathode electrode. During the transportation of the fuel to the flow channel plates, the redox reaction occurred on the anode/cathode electrode surfaces. As the fuel reached the outlet of the channel plate, the cotton in RE3 pushed it away from the cell by the same capillary force. By recording the elapsed time for a determined amount of the fuel (e.g., 500 mm^3) to flow through the cell, the flow rate can be calculated. The flow fields of the channel plates designed as the parallel type consisting of 27 channels, as shown in Table S1, were fabricated using a lithography technique.[49]

2.4. Characterization. To analyze the surface morphology and the chemical structure of the GOx immobilized on the bioanodic electrodes, field-emission scanning electron microscopy (FE-SEM) (JEOL, JSM-7600F) and Fourier-transform infrared spectroscopy (FTIR) (Bruker, Hyperion 3000/Vertex 70V) were carried out, respectively. Ultraviolet−visible (UV−vis) spectroscopy was used to analyze the amount of GOx immobilization on the scaffold electrode. To study the electrochemical property, cyclic voltammetry (CV) was conducted at room temperature by a program-controlled computer connected to the potentiostat (SP-240, Bio Logic). A three-electrode cell composed of a Pt counter electrode, a Ag/AgCl reference electrode (soaked in a 3.0 M solution of sodium chloride), and a working electrode was immersed into an electrolyte of 0.1 M $C_6H_{12}O_6$ in PBS (pH 7). The working electrodes of GOx[CS/TPP], GOx[CS/Na], and GOx[CS/TPP/Na] were prepared by dropping 20 μL of their biocatalyst solutions on glassy carbon electrodes (GCE) and these three biocatalyst electrodes were naturally dried at room temperature for 1 h. The self-pumping EBFC was examined by a fuel cell test station (EL505R3) for performance and stability tests.

3. RESULTS AND DISCUSSION

3.1. Surface Morphology of Different Bioanodic Electrodes. The schematic illustrations for formation of the bioanodic electrodes of GOx[CS/TPP]CC, GOx[CS/Na]CC, and GOx[CS/TPP/Na]CC by our fabrication processes, as mentioned in Section 2.2, are displayed in Figure 2a,e,i, respectively. The SEM images of Figure 2b,c,f,g,j,k illustrate the surface morphologies of [CS/TPP]CC, [CS/Na]CC, and [CS/TPP/Na]CC scaffolds, respectively. The SEM images of Figure 2d,h,l, show the surface morphologies of GOx[CS/TPP]CC, GOx[CS/Na]CC, and GOx[CS/TPP/Na]CC, respectively. The result indicates that the immobilization of GOx strongly relies on the scaffold structures of [CS/TPP], [CS/Na], and [CS/TPP/Na] on top of CC, suggesting that

https://dx.doi.org/10.1021/acs.energyfuels.0c01033
Energy Fuels 2020, 34, 10050−10058

the coated scaffolds can play a crucial part in exhibiting the catalytic ability of the immobilized GOx. In addition, it is found that GOx[CS/TPP]CC in Figure 2d (Figure S8a,b) shows a higher GOx immobilization than that of GOx[CS/Na]CC in Figure 2h (Figure S8c,d). Such a result can be ascribed to the formation of a porous microstructure of a cross-linked [CS/TPP] scaffold on CC, enabling the immobilization of GOx via the physical adsorption between negative GOx and positive CS. In contrast, the [CS/Na] without cross-linked TPP forms a gel embedded with CS, blocking the possibility to react with GOx, and also presents the tendency of peeling off. In Figure 2l (Figure S8e,f), however, the scaffold structure of [CS/TPP/Na], prepared by the combination of cross-linked [CS/TPP] with the addition of Na, exhibits a higher loading of GOx uniformly immobilized on CC than that of [CS/TPP]. This result suggests that combining [CS/Na] biopolymers with cross-linking [CS/TPP] to form a suitable porous scaffold with robust adhesion on CC can be beneficial for the enzyme immobilization, thereby prohibiting the release of the enzyme during the operation of the EBFC.

3.2. Chemical Structure of Bioanodic Electrodes. To understand the effect of a scaffold structure on the immobilized GOx, the chemical structures of [CS/TPP]CC, [CS/Na]CC, and [CS/TPP/Na]CC before and after immobilizing GOx were analyzed by FTIR, as shown in Figure 3. For the electrodes before the immobilization of GOx, the broad peaks at 3432 cm^{-1} and the peaks at around 2900 cm^{-1} belong to the O−H bonds and C−H stretching of the CS, respectively.[54,55]

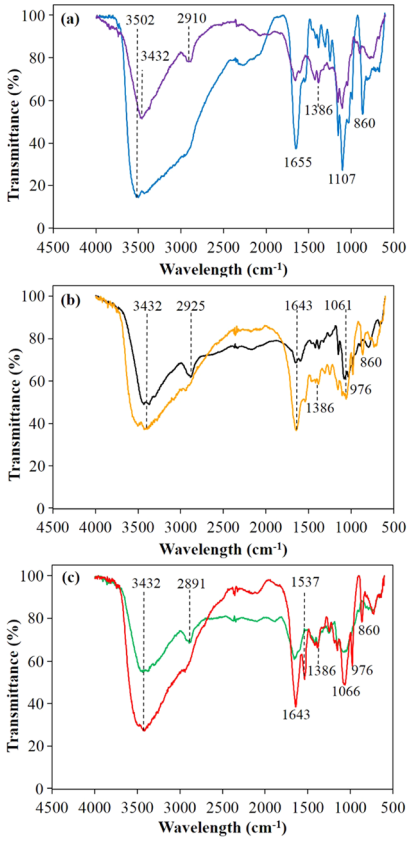

Figure 3. FTIR spectra of (a) [CS/TPP]CC (purple line) and GOx[CS/TPP]CC (blue line), (b) [CS/Na]CC (black line) and GOx[CS/Na]CC (orange line), and (c) [CS/TPP/Na]CC (green line) and GOx[CS/TPP/Na]CC (red line).

In addition, the C−O−C asymmetric bond from 1061 to 1107 cm^{-1} and the C═O double bond at 1643 cm^{-1} were also observed for the CS. For the electrodes after the immobilization of GOx, the FTIR peaks between 860 and 1100 cm^{-1} observed in GOx[CS/TPP]CC (blue line of Figure 3a), GOx[CS/Na]CC (orange line of Figure 3b), and GOx[CS/TPP/Na]CC (red line of Figure 3c) can be attributed to the phosphate buffer in the enzyme solution.[25] It can also be observed in all of the electrodes that the C−H stretching has disappeared, whereas the intensity of O−H stretching becomes stronger because of the O−H vibration of GOx. The typical strong absorption peaks at 1643 and 1655 cm^{-1} correspond to the C═O bond (amide I) of GOx due to the overlapping of the slight peaks of amide I band of CS.[56,57] Particularly, the amide II (N−H of GOx) band of GOx[CS/TPP/Na]CC at 1537 cm^{-1} is clearly observed while there is a weak peak found in the GOx[CS/TPP]CC and GOx[CS/Na]CC.[58,59] This result could suggest that GOx[CS/TPP/Na]CC has a higher loading of GOx than GOx[CS/Na]CC and GOx[CS/TPP]CC.

3.3. Amount of GOx Immobilized on Bioanodic Electrodes. To further understand the effect of a scaffold structure on the amount of immobilized GOx, the UV−vis spectrophotometry was applied to analyze the GOx concentration in the GOx solution before and after conducting the GOx immobilization process on various scaffolds of [CS/TPP/Na]CC, [CS/TPP]CC, and [CS/Na]CC. The low absorbance peak obtained for the GOx solution after the immobilization process indicates a large amount of GOx immobilized on the scaffold-decorated CC. To quantify the values of the GOx immobilized on the scaffold-decorated CC surface, the equation $C_{immobilization} = C_{total} - C_{residue}$ is used, where the $C_{immobilization}$, C_{total}, and $C_{residue}$ stand for the amount of GOx immobilized on the scaffold-decorated CC surface, the total amount of GOx in the original activated solution before immobilization, and the amount of GOx left in the solution after immobilization, respectively.[60,61] The UV−vis absorption spectra of all of the samples have a peak at around 260 nm, identified as the polypeptide chains of GOx in the solution.[62−64] All of the values of $C_{immobilization}$, C_{total}, and $C_{residue}$ can be deduced from the calibration curve, as shown in Figure S7, presenting the absorbance of 260 nm as a function of the GOx concentration. By comparing the total amount of GOx in the original activated solution and the residual amount of GOx in the solution after immobilization as shown in Figure 4, it can be noted that the GOx[CS/TPP/Na]CC sample has a higher amount of immobilized GOx (23.01 mg/6 cm^2) than

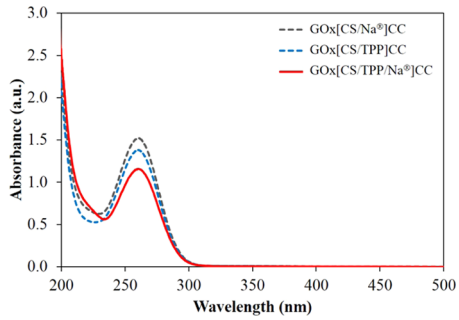

Figure 4. UV−vis spectra of the GOx solution after the immobilization of GOx on [CS/Na]CC, [CS/TPP]CC, and [CS/TPP/Na]CC.

https://dx.doi.org/10.1021/acs.energyfuels.0c01033
Energy Fuels 2020, 34, 10050−10058

that of GOx[CS/TPP]CC (19.53 mg/6 cm^2) and GOx[CS/Na]CC (17.3 mg/6 cm^2). This result confirms that the cross-linked [CS/TPP] with a Na polymer can provide a high loading of the enzyme on the conductive CC electrode due to its desirable scaffold.

3.4. Electrochemical Characterization of Bioanodic Electrodes. To understand the relationship between GOx and [CS/TPP/Na], a series of GOx[CS/TPP/Na] biocatalysts, prepared by adding different amounts of Na solution, on GCE were examined by the CV measurement under 0.1 M glucose at a 100 mV s^{-1} scan rate, as seen in Figure 5a, and the

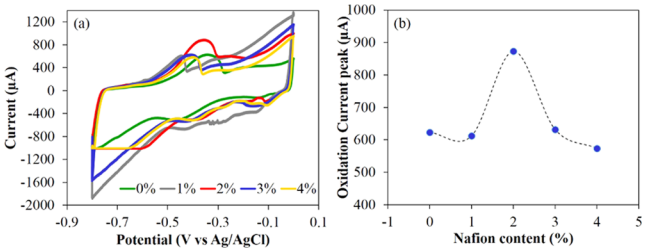

Figure 5. (a) CV of GOx[CS/TPP/Na] with different contents of Nafion on GCEs operated under a glucose concentration of 0.1 M PBS (pH 7) at 100 mV s^{-1} and the (b) corresponding plot of the oxidation current peak vs Nafion content.

corresponding plot of the oxidation current peak vs Nafion content, as shown in Figure 5b. It can be noted that the oxidation current peak of the GOx[CS/TPP/Na] catalyst at around −0.4 V is linearly increased from 624 to 876 μA with increase in the Nafion content from 0 to 2% and then reduced to 574 μA (4% of Nafion content). Such a trend suggests that the proper addition of Nafion content in cross-linked CS/TPP can help to form a more robust and protected scaffold structure to provide more sites for the immobilization of GOx, as well as be beneficial for the interaction between the surface electrode and GOx. The excess of Nafion content could easily make the scaffold flake off, as shown in Figure 2f, and potentially block the immobilized site of GOx on CS/TPP scaffold, leading to a poor electrochemical property.

The CV measurement of GOx[CS/TPP], GOx[CS/Na], and GOx[CS/TPP/Na] on GCEs operated under 0.1 M glucose at changed scan rates of 60, 80, and 100 mV s^{-1} is shown in Figure 6a−c, respectively, and their corresponding plot of oxidation current peaks vs various scan rates is indicated in Figure 6d. It can be observed that the oxidation current peak intensity is linearly raised by increasing the scan rate for all of the three electrodes. These trends can be attributed to the surface reaction-controlled reaction.[65,66] Moreover, the GOx[CS/TPP/Na] catalyst on GCE at a scan rate changed from 60 to 100 mV s^{-1} shows a highest redox current peak of 367−876 μA, as compared with GOx[CS/TPP] (182−624 μA) and GOx[CS/Na] (129−496 μA), respectively. This result suggests that a [CS/TPP/Na] scaffold embedded with a high loading of GOx can also exhibit a better electrochemical property.

3.5. EBFC Performance Using Different Bioanodic Electrodes. To further investigate the effect of a series of bioanodic electrodes on EBFC performance, the polarization curves of the EBFCs utilizing GOx[CS/TPP]CC, GOx[CS/Na]CC, and GOx[CS/TPP/Na]CC were obtained, as shown in Figure 7. The average flow rates of 0.499 μL s^{-1} (0.1 M $C_6H_{12}O_6$) and 0.764 μL s^{-1} (0.1 M $K_3Fe(CN)_6$) were

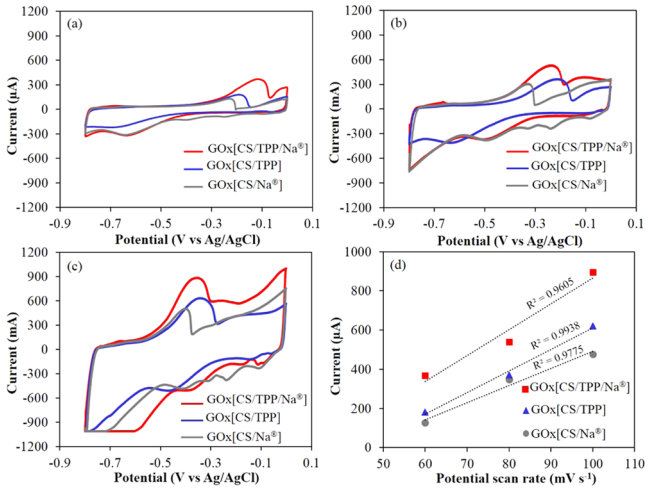

Figure 6. CV of GOx[CS/TPP], GOx[CS/Na], and GOx[CS/TPP/Na] biocatalysts on GCEs operated under a glucose concentration of 0.1 M PBS (pH 7) at various scan rates of (a) 60 mV s^{-1}, (b) 80 mV s^{-1}, and (c) 100 mV s^{-1} and (d) their corresponding plot of the oxidation current peak vs the scan rate.

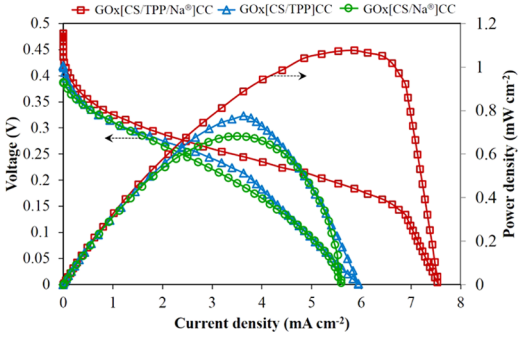

Figure 7. Performance of the self-pumping EBFC adopting various bioanodic electrodes of GOx[CS/TPP/Na]CC, GOx[CS/Na]CC, and GOx[CS/TPP]CC tested using a 0.1 M $C_6H_{12}O_6$ solution (PBS, pH 7) with 0.499 μL s^{-1} flow rate at the anodic side and a 0.1 M $K_3Fe(CN)_6$ solution with 0.764 μL s^{-1} flow rate at the cathodic side.

obtained due to automatic flow through the channel plate to the anode side and the cathode side, respectively, by the capillary force during the operation, as displayed in Figure S9. Our result shows that the maximum power density (MPD) of the self-pumping EBFC adopting GOx[CS/TPP/Na]CC is 1.077 mW cm^{-2}, which is higher than that of GOx[CS/TPP]CC (0.776 mW cm^{-2}) and GOx[CS/Na]CC (0.682 mW cm^{-2}). Such an improvement of around 57% can be mainly attributed to the capability of cross-linked CS/TPP matrices combined with Na polymers, providing the combined advantages of physical adsorption between CS and GOx[67,68] as well as the entrapment of cross-linked CS/TPP matrices[69] and Na polymer for the immobilization of GOx on CC.[70,71]

On the other hand, it can be particularly observed that the mass transport loss becomes significant at the GOx[CS/TPP/Na]CC electrode with the high GOx loading when the self-pumping EBFC is operated at the current density higher than 7 mA cm^{-2}. This result could be attributed to the finite mass transport rates of the species to or from the electrode through the capillary force during the operation. However, the EBFC developed by us adopting GOx[CS/TPP/Na]CC still shows a comparable power density to previously reported EBFCs, as

https://dx.doi.org/10.1021/acs.energyfuels.0c01033
Energy Fuels 2020, 34, 10050−10058

Table 1. Reported Performance of EBFCs

biofuel cell						
anode	cathode	OCP (V)	fuel (mM) (glucose)	power density (mW cm^{-2})	driving force/flow rate	ref
GOx/CNT	Laccase/CNT	0.94	50	1.30	N/A	22
GOx/GO/$Co(OH)_2$/CS	Lac/GO/$Co(OH)_2$/CS	0.46	100	0.52	N/A	23
TPA/[GOx/PEI/CNT]	Pt/C	0.46	200	0.98	60 mL/min	26
Pt/C	GA/[CNT/Lac/PEI/Lac]	0.40	40	0.20	100 mL/min	27
(GOx-GMC)/Na	Pt/C	0.24	10	0.02	peristaltic pump	28
MWCNT-COOH/Ni complex	CC	0.60	200 (sucrose)	0.41	N/A	75
Na/MWCNT/MG	CC	0.69		0.21		
EGDGE/ PEI/MWCNT	BOx/MWCNT/Nafion	0.71	5	0.03	2.55 μL/s	76
GOx[CS/TPP/Na]CC	$K_3Fe(CN)_6$ /CC	0.48	100	1.08	self-pumping	this work
GOx[CS/Na]CC	$K_3Fe(CN)_6$ /CC	0.39	100	0.68	self-pumping	this work
GOx[CS/TPP]CC	$K_3Fe(CN)_6$ /CC	0.42	100	0.78	self-pumping	this work

summarized in Table 1, suggesting the feasibility of achieving self-pumping EBFCs with high performance by optimizing the design of electrodes.

3.6. Stability of Enzymatic Biofuel Cells Using Various Bioanodic Electrodes. As shown in Figure 8, the stability

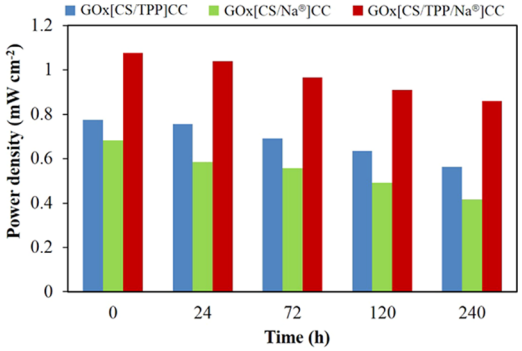

Figure 8. Stability performance of the self-pumping EBFC utilizing GOx[CS/TPP]CC, GOx[CS/Na]CC, and GOx[CS/TPP/Na]CC as the bioanodic electrodes operated at room temperature after 0, 24, 72, 120, and 240 h.

performance of the self-pumping EBFC adopting GOx[CS/TPP]CC, GOx[CS/Na]CC, and GOx[CS/TPP/Na]CC electrodes working after 0, 24, 72, 120, and 240 h was evaluated. The result illustrates that the MPD of a self-pumping EBFC utilizing GOx[CS/TPP/Na]CC is reduced from 96.6% (24 h) to 89.2% (240 h) of its beginning value whereas that of the EBFC utilizing GOx[CS/TPP]CC and GOx[CS/Na]CC is declined from 97.3% (24 h) to 79.9% (240 h) and from 85.9% (24 h) to 61.1% (240 h) of their beginning values, respectively. Such a declining trend could be mostly ascribed to the exfoliation of GOx[72−74] and the degradation of the enzyme by H_2O_2 with time.[72,73] Consequently, our self-pumping EBFC utilizing GOx[CS/TPP/Na]CC shows the best stability as compared with that utilizing GOx[CS/TPP]CC and GOx[CS/Na]CC, indicating that the coated scaffolds composed of hybrid enzyme immobilization approaches also play a crucial part in sustaining the GOx catalytic ability during the long-time operation.

4. CONCLUSIONS

The effect of bioanodic electrodes with different scaffold structures on the self-pumping EBFC performance has been investigated systematically. A series of bioanodic electrodes, such as GOx[CS/TPP]CC, GOx[CS/Na]CC, and GOx[CS/TPP/Na]CC, were prepared to understand the effect of the scaffold structure composed of TPP, Na, and CS on the GOx immobilized on CC. It was found that a preferred scaffold decorated on the CC can be achieved by a hybrid approach of cross-linked [CS/TPP] matrices with proper Na polymers, not only improving the enzyme-loading efficiency but also facilitating the interaction between the surface electrode and GOx. The excess of Nafion content could easily make the scaffold flake off and constrain the immobilized GOx, leading to a poor electrochemical property. Our result reveals that the self-pumping EBFC adopting GOx[CS/TPP/Na]CC can deliver a higher peak power density (1.077 mW cm^{-2}) than that utilizing GOx[CS/TPP]CC (0.776 mW cm^{-2}) and GOx[CS/Na]CC (0.682 mW cm^{-2}). The self-pumping EBFC utilizing GOx[CS/TPP/Na]CC can retain 89.2% of its beginning performance even after 240 h of stable testing, as compared with that of utilizing GOx[CS/Na]CC (61.1%). Such an enhancement via the designed scaffold structures on the electrode can provide insight into the feasibility of high-performance and long-lifetime self-pumping EBFC.

■ ASSOCIATED CONTENT

Supporting Information

The Supporting Information is available free of charge at https://pubs.acs.org/doi/10.1021/acs.energyfuels.0c01033.

Ionic interaction of the crosslinking, cross-linked chitosan and GOx enzyme immobilization mechanism, scheme of the single enzyme-based biofuel cell system, configuration of single self-pumping EBFC, size of each channel in the fluid plate, channel plate design of self-pumping EBFC, top/bottom end plates of the self-pumping EBFC and its entity diagram, calibration curve of the absorbance as a function of GOx concentration, flow rate of the fuel at the anode/cathode in the self-pumping EBFC (PDF)

■ AUTHOR INFORMATION

Corresponding Authors

Chih-Liang Wang − *Graduate Institute of Precision Engineering, National Chung Hsing University, Taichung City 402, Taiwan;* orcid.org/0000-0002-0772-4285; Email: clwang@email.nchu.edu.tw

Hsiharng Yang − *Graduate Institute of Precision Engineering and Innovation and Development Center of Sustainable*

https://dx.doi.org/10.1021/acs.energyfuels.0c01033
Energy Fuels 2020, 34, 10050−10058

Agriculture (IDCSA), National Chung Hsing University, Taichung City 402, Taiwan; Email: hsiharng@dragon.nchu.edu.tw

Authors

Ngoc Bich Duong − *Graduate Institute of Precision Engineering, National Chung Hsing University, Taichung City 402, Taiwan; School of Agriculture and Aquaculture, Tra Vinh University, Tra Vinh 87000, Vietnam*

Van Men Truong − *Graduate Institute of Precision Engineering, National Chung Hsing University, Taichung City 402, Taiwan; School of Engineering and Technology, Tra Vinh University, Tra Vinh 87000, Vietnam*

Yi-Shiuan Li − *Graduate Institute of Precision Engineering, National Chung Hsing University, Taichung City 402, Taiwan*

Complete contact information is available at: https://pubs.acs.org/10.1021/acs.energyfuels.0c01033

Notes

The authors declare no competing financial interest.

■ ACKNOWLEDGMENTS

This work was funded by the Ministry of Science and Technology of Taiwan (grant number: MOST-108-2221-E-005-026) and also partially supported by the Ministry of Education, Taiwan, R.O.C. under the Higher Education Sprout Project.

■ REFERENCES

(1) Perera, F. Pollution from Fossil-Fuel Combustion is the Leading Environmental Threat to Global Pediatric Health and Equity: Solutions Exist. *Int. J. Environ. Res. Public Health* **2017**, *15*, No. 16.

(2) Anderson, T. R.; Hawkins, E.; Jones, P. D. CO2, the greenhouse effect and global warming: from the pioneering work of Arrhenius and Callendar to today's Earth System Models. *Endeavour* **2016**, *40*, 178−187.

(3) Kumar, A.; Sharma, S.; Pandey, L. M.; Chandra, P. Nano-engineered material based biosensing electrodes for enzymatic biofuel cells applications. *Mater. Sci. Energy Technol.* **2018**, *1*, 38−48.

(4) Rasmussen, M.; Abdellaoui, S.; Minteer, S. D. Enzymatic biofuel cells: 30 years of critical advancements. *Biosens. Bioelectron.* **2016**, *76*, 91−102.

(5) Le Goff, A.; Holzinger, M. Molecular engineering of the bio/nano-interface for enzymatic electrocatalysis in fuel cells. *Sustainable Energy Fuels* **2018**, *2*, 2555−2566.

(6) Robinson, P. Enzymes: principles and biotechnological applications. *Essays Biochem.* **2015**, *59*, 1−41.

(7) Eisenthal, R.; Peterson, M.; Daniel, R.; Danson, M. The thermal behaviour of enzyme activity: Implications for biotechnology. *Trends Biotechnol.* **2006**, *24*, 289−92.

(8) de Andrades, D.; Graebin, N. G.; Kadowaki, M. K.; Ayub, M. A. Z.; Fernandez-Lafuente, R.; Rodrigues, R. C. Immobilization and stabilization of different β-glucosidases using the glutaraldehyde chemistry: Optimal protocol depends on the enzyme. *Int. J. Biol. Macromol.* **2019**, *129*, 672−678.

(9) Gellett, W.; Kesmez, M.; Schumacher, J.; Akers, N.; Minteer, S. D. Biofuel Cells for Portable Power. *Electroanalysis* **2010**, *22*, 727−731.

(10) MacVittie, K.; Halámek, J.; Halámková, L.; Southcott, M.; Jemison, W.; Lobel, R.; Katz, E. From "cyborg" lobsters to a pacemaker powered by implantable biofuel cells. *Energy Environ. Sci.* **2013**, *6*, 81−86.

(11) Sales, C. P. F.; Iost, R.; Martins, M.; Almeida, M.; Crespilho, F. An intravenous implantable glucose/dioxygen biofuel cell with modified flexible carbon fiber electrodes. *Lab Chip* **2012**, *13*, 468−474.

(12) Cosnier, S.; Le Goff, A.; Holzinger, M. Towards glucose biofuel cells implanted in human body for powering artificial organs: Review. *Electrochem. Commun.* **2014**, *38*, 19−23.

(13) Katz, E.; Bückmann, A. F.; Willner, I. Self-Powered Enzyme-Based Biosensors. *J. Am. Chem. Soc.* **2001**, *123*, 10752−10753.

(14) Amir, L.; Tam, T. K.; Pita, M.; Meijler, M. M.; Alfonta, L.; Katz, E. Biofuel Cell Controlled by Enzyme Logic Systems. *J. Am. Chem. Soc.* **2009**, *131*, 826−832.

(15) Huang, X.; Zhang, L.; Zhang, Z.; Guo, S.; Shang, H.; Li, Y.; Liu, J. Wearable biofuel cells based on the classification of enzyme for high power outputs and lifetimes. *Biosens. Bioelectron.* **2019**, *124-125*, 40−52.

(16) Hestekin, J.; Lin, Y. P.; Frank, J. R.; Snyder, S.; Martin, E. J. Electrochemical enhancement of glucose oxidase kinetics: Gluconic acid production with anion exchange membrane reactor. *J. Appl. Electrochem.* **2002**, *32*, 1049−1052.

(17) Wang, C.-T.; Chen, W.-J.; Huang, R.-Y. Influence of growth curve phase on electricity performance of microbial fuel cell by *Escherichia coli*. *Int. J. Hydrogen Energy* **2010**, *35*, 7217−7223.

(18) Justin, G. A.; Yingze, Z.; Mingui, S.; Sclabassi, R. *Biofuel Cells: A Possible Power Source for Implantable Electronic Devices*, The 26th Annual International Conference of the IEEE Engineering in Medicine and Biology Society, Sept 1−5, 2004; pp 4096−4099.

(19) Pereira, A. R.; Sedenho, G. C.; Souza, J. C. P. D.; Crespilho, F. N. Advances in enzyme bioelectrochemistry. *An. Acad. Bras. Cienc.* **2018**, *90*, 825−857.

(20) Ferapontova, E. E.; Shleev, S.; Ruzgas, T.; Stoica, L.; Christenson, A.; Tkac, J.; Yaropolov, A. I.; Gorton, L. Direct Electrochemistry of Proteins and Enzymes. In *Perspectives in Bioanalysis*, Paleček, E.; Scheller, F.; Wang, J., Eds.; Elsevier, 2005; Vol. *1*, pp 517−598.

(21) Chen, X.; Jia, J.; Dong, S. Organically Modified Sol-Gel/Chitosan Composite Based Glucose Biosensor. *Electroanalysis* **2003**, *15*, 608−612.

(22) Zebda, A.; Gondran, C.; Le Goff, A.; Holzinger, M.; Cinquin, P.; Cosnier, S. Mediatorless high-power glucose biofuel cells based on compressed carbon nanotube-enzyme electrodes. *Nat. Commun.* **2011**, *2*, No. 370.

(23) Uk Lee, H.; Young Yoo, H.; Lkhagvasuren, T.; Seok Song, Y.; Park, C.; Kim, J.; Wook Kim, S. Enzymatic fuel cells based on electrodeposited graphite oxide/cobalt hydroxide/chitosan composite−enzymeelectrode. *Biosens. Bioelectron.* **2013**, *42*, 342−348.

(24) Zebda, A.; Tingry, S.; Innocent, C.; Cosnier, S.; Forano, C.; Mousty, C. Hybrid layered double hydroxides-polypyrrole composites for construction of glucose/O2 biofuel cell. *Electrochim. Acta* **2011**, *56*, 10378−10384.

(25) Falk, M.; Blum, Z.; Shleev, S. Direct electron transfer based enzymatic fuel cells. *Electrochim. Acta* **2012**, *82*, 191−202.

(26) Chung, Y.; Ahn, Y.; Christwardana, M.; Kim, H.; Kwon, Y. Development of a glucose oxidase-based biocatalyst adopting both physical entrapment and crosslinking, and its use in biofuel cells. *Nanoscale* **2016**, *8*, 9201−9210.

(27) Christwardana, M. Combination of physico-chemical entrapment and crosslinking of low activity laccase-based biocathode on carboxylated carbon nanotube for increasing biofuel cell performance. *Enzyme Microb. Technol.* **2017**, *106*, 1−10.

(28) Garcia-Perez, T.; Hong, S.-G.; Kim, J.; Ha, S. Entrapping cross-linked glucose oxidase aggregates within a graphitized mesoporous carbon network for enzymatic biofuel cells. *Enzyme Microb. Technol.* **2016**, *90*, 26−34.

(29) Susanto, H.; Samsudin, A. M.; Rokhati, N.; Widiasa, I. N. Immobilization of glucose oxidase on chitosan-based porous composite membranes and their potential use in biosensors. *Enzyme Microb. Technol.* **2013**, *52*, 386−392.

(30) Cao, L. Unconventional Enzyme Immobilization. In *Carrier-Bound Immobilized Enzymes*, 2006; pp 449−549.

(31) Catalano, P. N.; Wolosiuk, A.; Soler-Illia, G. J. A. A.; Bellino, M. G. Wired enzymes in mesoporous materials: A benchmark for fabricating biofuel cells. *Bioelectrochemistry* **2015**, *106*, 14−21.

(32) Schoevaart, R.; Wolbers, M.; Golubovic, M.; Ottens, M.; Kieboom, A.; Rantwijk, F.; Wielen, L.; Sheldon, R. Preparation, optimization, and structures of cross-linked enzyme aggregates (CLEAs). *Biotechnol. Bioeng.* **2004**, *87*, 754−62.
(33) Takigawa, T.; Endo, Y. Effects of Glutaraldehyde Exposure on Human Health. *J. Occup. Health* **2006**, *48*, 75−87.
(34) Nasution, T. I.; Asrosa, R.; Nainggolan, I.; Balyan, M.; Indah, R.; Wahyudi, A. Sodium tripolyphosphate cross-linked chitosan based sensor for enhacing sensing properties towards acetone. *IOP Conf. Ser.: Mater. Sci. Eng.* **2018**, *309*, No. 012083.
(35) Kucukkolbasi, S.; Erdoğan, Z. O.; Barek, J.; Sahin, M.; Kocak, N. A novel chitosan nanoparticle-schiff base modified carbon paste electrode as a sensor for the determination of Pb(II) in waste water. *Int. J. Electrochem. Sci.* **2013**, *8*, 2164−2181.
(36) Klotzbach, T. L.; Watt, M.; Ansari, Y.; Minteer, S. D. Improving the microenvironment for enzyme immobilization at electrodes by hydrophobically modifying chitosan and Nafion polymers. *J. Membr. Sci.* **2008**, *311*, 81−88.
(37) Tan, Y.; Deng, W.; Ge, B.; Xie, Q.; Huang, J.; Yao, S. Biofuel cell and phenolic biosensor based on acid-resistant laccase−glutaraldehyde functionalized chitosan−multiwalled carbon nanotubes nanocomposite film. *Biosens. Bioelectron.* **2009**, *24*, 2225−2231.
(38) Huang, Y.; Qin, X.; Li, Z.; Fu, Y.; Qin, C.; Wu, F.; Su, Z.; Ma, M.; Xie, Q.; Yao, S.; Hu, J. Fabrication of a chitosan/glucose oxidase−poly(anilineboronic acid)−Aunano/Au-plated Au electrode for biosensor and biofuel cell. *Biosens. Bioelectron.* **2012**, *31*, 357−362.
(39) Kang, S.; Hyun, K.; Chung, Y.; Kwon, Y. A biocatalyst containing chitosan and embedded dye mediator adopted for promoting oxidation reactions and its utilization in biofuel cells. *Appl. Surf. Sci.* **2020**, *507*, No. 145007.
(40) Wang, X.; Kim, S. B.; Khang, D.; Kim, H.-H.; Kim, C.-J. Optimization and characterization of covalent immobilization of glucose oxidase for bioelectronic devices. *Biochem. Eng. J.* **2016**, *112*, 20−31.
(41) Hassani, S.; Laouini, A.; Fessi, H.; Charcosset, C. Preparation of chitosan−TPP nanoparticles using microengineered membranes − Effect of parameters and encapsulation of tacrine. *Colloids Surf., A* **2015**, *482*, 34−43.
(42) Liu, C.; Bai, R.; Nan, L. In *Sodium Tripolyphosphate (TPP) Crosslinked Chitosan Membranes and Application in Humic Acid Removal*, AIChE Annual Meeting, 2004; Conference Proceedings, 2004; pp 5561−5574.
(43) Shrestha, B. K.; Ahmad, R.; Mousa, H. M.; Kim, I.-G.; Kim, J. I.; Neupane, M. P.; Park, C. H.; Kim, C. S. High-performance glucose biosensor based on chitosan-glucose oxidase immobilized polypyrrole/Nafion/functionalized multi-walled carbon nanotubes bionanohybrid film. *J. Colloid Interface Sci.* **2016**, *482*, 39−47.
(44) Jayakumar, R.; Prabaharan, M.; Nair, S. V.; Tamura, H. Novel chitin and chitosan nanofibers in biomedical applications. *Biotechnol. Adv.* **2010**, *28*, 142−150.
(45) Koev, S. T.; Dykstra, P. H.; Luo, X.; Rubloff, G.; E Bentley, W.; F Payne, G.; Ghodssi, R. Chitosan: An integrative biomaterial for lab-on-a-chip devices. *Lab Chip* **2010**, *10*, 3026−3042.
(46) El Ichi, S.; Marzouki, M. N.; Korri-Youssoufi, H. Direct monitoring of pollutants based on an electrochemical biosensor with novel peroxidase (POX1B). *Biosens. Bioelectron.* **2009**, *24*, 3084−3090.
(47) Halámková, L.; Halámek, J.; Bocharova, V.; Szczupak, A.; Alfonta, L.; Katz, E. Implanted biofuel cell operating in a living snail. *J. Am. Chem. Soc.* **2012**, *134*, 5040−5043.
(48) El Ichi-Ribault, S.; Alcaraz, J.-P.; Boucher, F.; Boutaud, B.; Dalmolin, R.; Boutonnat, J.; Cinquin, P.; Zebda, A.; Martin, D. K. Remote wireless control of an enzymatic biofuel cell implanted in a rabbit for 2 months. *Electrochim. Acta* **2018**, *269*, 360−366.
(49) Tsai, Y.-F.; Shieh, C.-J.; Yang, H. Capillary force pumping fluid for glucose oxidase enzymatic fuel cells. *Microsyst. Technol.* **2015**, *23*, 3927−3935.
(50) Duong, N. B.; You, S. L.; Huang, L. Z.; Yang, H. Carbon Nanotubes Modified Carbon Cloth Cathode Electrode for Self-Pumping Enzymatic Biofuel Cell. *J. Renewable Energy* **2018**, *2018*, 1−8.
(51) Carmo, M.; Brandalise, M.; Neto, A. O.; Spinacé, E. V.; Taylor, A. D.; Linardi, M.; Rocha Poço, J. G. Enhanced activity observed for sulfuric acid and chlorosulfuric acid functionalized carbon black as PtRu and PtSn electrocatalyst support for DMFC and DEFC applications. *Int. J. Hydrogen Energy* **2011**, *36*, 14659−14667.
(52) Kuo, C.-H.; Huang, W. H.; Lee, C.-K.; Liu, Y. C.; Chang, J. C. M.; Yang, H.; Shieh, C. J. Biofuel Cells Composed by Using Glucose Oxidase on Chitosan Coated Carbon Fiber Cloth. *Int. J. Electrochem. Sci.* **2013**, *8*, 9242−9255.
(53) Duong, N. B.; Wang, C.-L.; Huang, L. Z.; Fang, W. T.; Yang, H. Development of a facile and low-cost chitosan-modified carbon cloth for efficient self-pumping enzymatic biofuel cells. *J. Power Sources* **2019**, *429*, 111−119.
(54) Rwegasila, E.; Mubofu, E. B.; Nyandoro, S. S.; Erasto, P.; Munissi, J. J. E. Preparation, characterization and in vivo antimycobacterial studies of panchovillin-chitosan nanocomposites. *Int. J. Mol. Sci.* **2016**, *17*, 1559.
(55) Dabóczi, M.; Albert, E.; Agócs, E.; Kabai-Faix, M.; Hórvölgyi, Z. Bilayered (silica−chitosan) coatings for studying dye release in aqueous media: The role of chitosan properties. *Carbohydr. Polym.* **2016**, *136*, 137−145.
(56) Wang, X.; Zhu, K.-X.; Zhou, H.-M. Immobilization of glucose oxidase in alginate-chitosan microcapsules. *Int. J. Mol. Sci.* **2011**, *12*, 3042−3054.
(57) Baghayeri, M. Glucose sensing by a glassy carbon electrode modified with glucose oxidase and a magnetic polymeric nanocomposite. *RSC Adv.* **2015**, *5*, 18267−18274.
(58) Delfino, I.; Portaccio, M.; Ventura, B. D.; Mita, D. G.; Lepore, M. Enzyme distribution and secondary structure of sol−gel immobilized glucose oxidase by micro-attenuated total reflection FT-IR spectroscopy. *Mater. Sci. Eng.: C* **2013**, *33*, 304−310.
(59) Chey, C.; Ibupoto, Z.; Khun, K.; Nur, O.; Willander, M., Indirect Determination of Mercury Ion by Inhibition of a Glucose Biosensor Based on ZnO Nanorods. *Sensors* 2012, *12*, 15063−77.
(60) Morshed, M. N.; Behary, N.; Bouazizi, N.; Guan, J.; Chen, G.; Nierstrasz, V. Surface modification of polyester fabric using plasma-dendrimer for robust immobilization of glucose oxidase enzyme. *Sci. Rep.* **2019**, *9*, No. 15730.
(61) Kahoush, M.; Behary, N.; Cayla, A.; Mutel, B.; Guan, J.; Nierstrasz, V. Surface modification of carbon felt by cold remote plasma for glucose oxidase enzyme immobilization. *Appl. Surf. Sci.* **2019**, *476*, 1016−1024.
(62) Tsai, T.-W.; Heckert, G.; Neves, L. F.; Tan, Y.; Kao, D.-Y.; Harrison, R. G.; Resasco, D. E.; Schmidtke, D. W. Adsorption of Glucose Oxidase onto Single-Walled Carbon Nanotubes and Its Application in Layer-By-Layer Biosensors. *Anal. Chem.* **2009**, *81*, 7917−7925.
(63) Shao, Q.; Wu, P.; Xu, X.; Zhang, H.; Cai, C. Insight into the effects of graphene oxide sheets on the conformation and activity of glucose oxidase: towards developing a nanomaterial-based protein conformation assay. *Phys. Chem. Chem. Phys.* **2012**, *14*, 9076−9085.
(64) Chung, R.-J.; Wang, A.-N.; Peng, S.-Y. An Enzymatic Glucose Sensor Composed of Carbon-Coated Nano Tin Sulfide. *Nanomaterials* **2017**, *7*, 39.
(65) Zhou, J.; Min, M.; Liu, Y.; Tang, J.; Tang, W. Layered assembly of NiMn-layered double hydroxide on graphene oxide for enhanced non-enzymatic sugars and hydrogen peroxide detection. *Sens. Actuators, B* **2018**, *260*, 408−417.
(66) Hu, Z. Direct Electron Transfer of Glucose Oxidase in Carbon Paper for Biofuel Cells and Biosensors. *Int. J. Electrochem. Sci.* **2017**, 7103−7120.
(67) Liu, Y.; Wang, M.; Zhao, F.; Xu, Z.; Dong, S. The direct electron transfer of glucose oxidase and glucose biosensor based on carbon nanotubes/chitosan matrix. *Biosens. Bioelectron.* **2005**, *21*, 984−988.
(68) Kang, X.; Wang, J.; Wu, H.; Aksay, I. A.; Liu, J.; Lin, Y. Glucose Oxidase−graphene−chitosan modified electrode for direct electro-

https://dx.doi.org/10.1021/acs.energyfuels.0c01033
Energy Fuels 2020, 34, 10050−10058

chemistry and glucose sensing. *Biosens. Bioelectron.* **2009**, *25*, 901−905.
(69) Bagal-Kestwal, D. R.; Chiang, B.-H. Exploration of Chitinous Scaffold-Based Interfaces for Glucose Sensing Assemblies. *Polymers* **2019**, *11*, No. 1958.
(70) Samir, S.; Mahmoud, Y.; Matter, I.; El-Samahy, T.; Darwesh, O. *Methods in Enzymology*, 1st ed.; Academic Press: United State, 2020; Vol. *630*.
(71) Ressam, I.; Krins, N.; Laberty-Robert, C.; Selmane, M.; Lahcini, M.; Raihane, M.; Kadib, A. E.; Perrot, H.; Sel, O. Sulfonic Acid Functionalized Chitosan as a Sustainable Component for Proton Conductivity Management in PEMs. *ChemistrySelect* **2017**, *2*, 2503−2511.
(72) Chung, Y.; Tannia, D. C.; Kwon, Y. Glucose biofuel cells using bi-enzyme catalysts including glucose oxidase, horseradish peroxidase and terephthalaldehyde crosslinker. *Chem. Eng. J.* **2018**, *334*, 1085−1092.
(73) Harris, J. M.; Reyes, C.; Lopez, G. P. Common Causes of Glucose Oxidase Instability in In Vivo Biosensing: A Brief Review. *J. Diabetes Sci. Technol.* **2013**, *7*, 1030−1038.
(74) Jia, W.; Jin, C.; Xia, W.; Muhler, M.; Schuhmann, W.; Stoica, L. Glucose Oxidase/Horseradish Peroxidase Co-immobilized at a CNT-Modified Graphite Electrode: Towards Potentially Implantable Biocathodes. *Chem. - Eur. J.* **2012**, *18*, 2783−2786.
(75) Zhang, Y.; Arugula, M. A.; Williams, S. T.; Minteer, S. D.; Simonian, A. L. Layer-by-layer assembly of carbon nanotubes modified with invertase/glucose dehydrogenase cascade for sucrose/o2 biofuel cell. *J. Electrochem. Soc.* **2016**, *163*, F449−F454.
(76) del Torno-de Román, L.; Navarro, M.; Hughes, G.; Esquivel, J. P.; Milton, R. D.; Minteer, S. D.; Sabaté, N. Improved performance of a paper-based glucose fuel cell by capillary induced flow. *Electrochim. Acta* **2018**, *282*, 336−342.

https://dx.doi.org/10.1021/acs.energyfuels.0c01033
Energy Fuels 2020, 34, 10050−10058